ESTIMATION OF THE RADIATION ENVIRONMENT BASED ON THE NASA AP-8 AND AE-8 MODELS

Thomas L. Morton
OAI
NASA Glenn Research Center
21000 Brookpark Rd, MS 302-1
Cleveland, OH 44135

ABSTRACT

In this paper, we discuss the earth's trapped radiation environment, as described by the NASA models AP-8 and AE-8. We include a description of the sources and structure of the trapped radiation belts, and their dependence on external factors. After describing how to use the models to predict the environment, we present data from various space missions, and compare those data to the models. This shows the limits and strengths of the models. Finally, we describe alternative models of the trapped radiation belts, and discuss why they have not been widely adopted yet.

1. Introduction

Since the dawn of the space age, scientists have known about the high-energy particles trapped in the earth's magnetosphere. During the 1960's and 1970's, NASA collected data from a large fleet of satellites which samples much of the trapped radiation belts, and developed various empirical models of the structure of those belts. The current versions of these models are AP-8 for trapped protons, and AE-8 for trapped electrons.

These models are based on observations from 43 satellites, and cover the times 1958-1970 for AP-8, and 1958- 1978 for AE-8.[1] They are based on a two-dimensional coordinate system, defined by the earth's magnetic field. The only time resolution in the models is a distinction between high and low solar activity. Each model generates a prediction of the average integral or differential flux expected over a six-month time period, so they do not predict fast time-scale phenomena.

To understand what the models provide, it is useful to understand the sources of the trapped particles. The major sources of the protons and electrons include the solar wind, diffusion from the polar ionosphere, acceleration from the magnetosheath, and Cosmic Ray albedo neutron decay (CRAND).[2] All of the sources are not known, nor do we understand how the particles are accelerated to such high energies. In any event, charged particles enter the earth's magnetic field, and are accelerated to the north (or south) along the field lines. Because the field is non-uniform, the particles "bounce" near the polar regions, and proceed back along the same field line. In addition, the electrons experience an eastward drift, and the positively charged ions experience a westward drift. This is shown schematically in Figure 1.

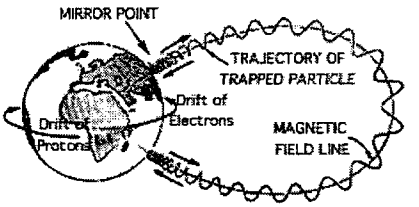

Figure 1 - Spiral trajectories bouncing in the earth's magnetic field

The earth's magnetic field is therefore the major driver of the belts. It consists of a dipolar component, and a dynamic field. The dipolar field is approximately .3 Gauss, and is slightly offset from the earth's center and rotation axis. The dynamic field results from the interaction of the dipole field and the sun's magnetic field, as transported by the solar wind. This field varies with the sun's activity, as the earth rotates, and as it revolves around the sun.

Solar activity is the other major driver of the belts. As the sun generates flares and coronal mass ejections, more particles are ejected, and the earth's magnetic field is compressed, so the structure of the belts changes. In addition, the sun's magnetic field, which flows with the solar wind, shields the earth from cosmic rays, which provide one of the sources of trapped particles. This primarily affects the outer radiation belts, since the inner belts are driven by the lower magnetic field, which is strongly shielded from the magnetopause.

The coordinates used for the magnetic field are the field strength, B, and the McIlwain L number. The L number was proposed by McIlwain[3] in 1961, as a means of organizing the early data from the experiments that measured trapped particles. It is defined by the lines of force in the magnetic field and scaled so that, at the magnetic equator, the L number is the distance from the center of the earth, in earth radii. These coordinates are sketched in Figure 2 for a pure dipole field. The AP-8 and AE-8 models use the scaled coordinate B/B_0, which is the ratio of the field strength to the field strength along the same L shell, at the magnetic equator. The dynamic field models are more complex, but are not needed for the AP-8 or AE-8 models.

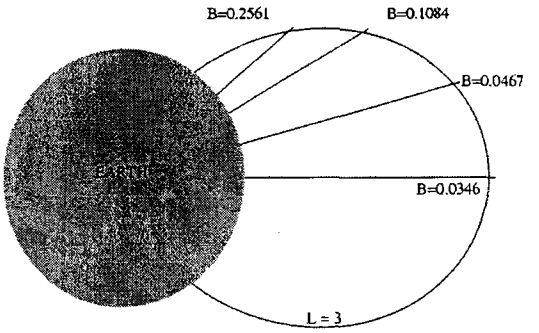

Figure 2 - Magnetic field B/L coordinate system

2. The AP-8 and AE-8 Models

AP-8 and AE-8 are the current NASA models for trapped radiation environments.[456] They can return an integral or differential omnidirectional flux for a set of energies. The integral flux is the number of particles with energy greater than or equal to the input energy. For the differential flux, the models calculate a numerical derivative of the integral flux. In each case, the models interpolate from an internal table, which lists integral fluxes for selected energies, indexed by L and B/B_0. Table 1 shows the energy ranges and parameter space covered by the models.

Table 1 - Ranges used in models

	AP-8	AE-8
Particle Type	Protons	Electrons
Energy Range	.1 – 400 MeV	.04 – 7 MeV
McIlwain L number	1.1 – 7	1.1 – 11

As we mentioned before, AP-8 returns the expected average flux for a six-month period. Therefore, it relies on the static magnetic field. In addition, since it is based on data from the 1960's and 1970's, it requires the magnetic field from that era. The models expect the Jensen and Cain models, but I have been able to use the IGRF from the NSSDC web-site with no difficulties. The models have a factor of two accuracy, but daily variation can be as much as a factor of ten from the models. In addition, during high solar activity, the electron densities can be off by a factor of 100 or more.

The NASA model for the internal dipole field is the International Geomagnetic Reference Field (IGRF)[7]. This model is a set of empirical coefficients for a sum of solid spherical harmonics and their derivatives, which describe the field. The magnetic field varies with time, so the coefficients also vary. The model is updated approximately every five years, to include the latest empirical field values, and to extrapolate for another five years into the future. The current version is IGRF-2000.[8] The model also provides the McIlwain L number, and the field strength B at a point near the earth. It requires the geographic latitude, longitude, and altitude as input.

The procedure for extracting an integral proton flux is to create an array of energies for which the fluxes are desired. In addition, it is necessary to initialize AP-8. This is a subroutine call which sets the

array of particle fluxes to use (in this case, protons or electrons, solar minimum or solar maximum), and to select a magnetic field. It is important to use the field for either 1964 (solar minimum) or 1970 (solar maximum). At each position in space (usually along an orbit), call the IGRF model with the geographic position, requesting the magnetic coordinates (i.e. McIlwain L number, and scaled field strength B/B_0). With these numbers, you have the inputs for the call to AP-8 which returns the integral flux for each input energy. A similar sequence of calls works for AE-8.

It is important to remember that the solar activity affects the radiation belts. In Figure 3, we show the sunspot number from 1950 until the present[9]. These data have been maintained since the 1600's, when Galileo discovered sunspots. We note that the 1970 solar max was unremarkable for the space age. Indeed, it was the smallest of the space age until the 2000 cycle. The full dependence of the particle flux on solar activity remains an open problem.

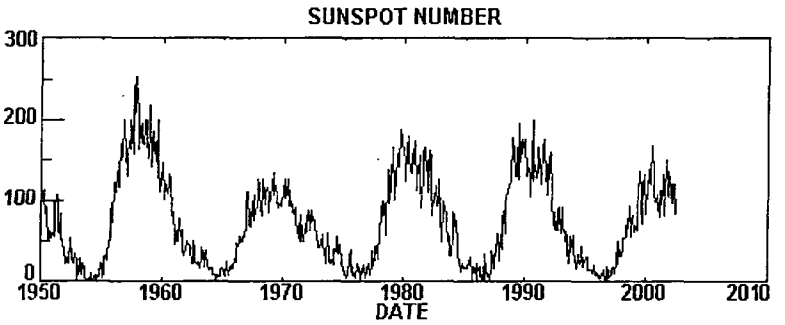

Figure 3 - Sunspot number since 1950

So what are the AP-8 and AE-8 models good for? They provide an average integral flux for a large fraction of the magnetosphere, including forth the solar minimum and solar maximum conditions. They are empirical, and cover a large energy range. Many of the sketches shown in the literature of the structure of the radiation belts are created using the AP-8 and AE-8 models. In Figure 4-5, we show a map of protons >10 MeV around the earth, and electrons > 1 MeV. The general belts are clearly visible, and the models provide a sense of which altitudes/orbits will sustain the greatest damage. For example, the proton flux peaks at an altitude of about .7 R_e, and the equatorial electrons show two peaks, at altitudes 1 and 4.R_e.

If the process being studied operates on a slow time scale (that is, weeks-years), then these models will provide adequate information. For example, radiation damage to solar cells is a relatively slow process, because the solar cells sustain relatively little damage each week. In addition, the damage roughly depends on the logarithm of the flux of particles. Here, we consider the solar arrays on the COMETS

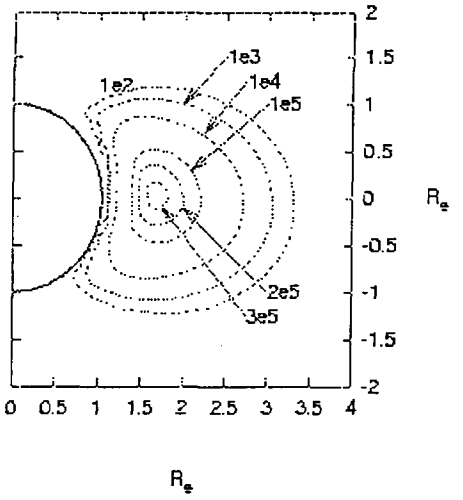

Figure 4 - Contour map of protons > 10 MeV near earth.

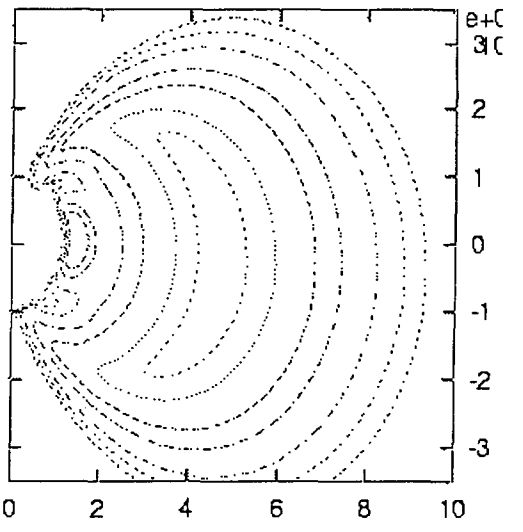

Figure 5 - Contour map of electrons > 1 MeV near earth.

mission. COMETS was a 1998 NASDA mission that failed to achieve its geosynchronous orbit. With some quick orbital changes, the satellite was placed into an elliptical orbit of about 500 x 17,000 km.[10] This exposed the solar arrays to heavy proton irradiation, instead of the mostly electron radiation expected at geosynchronous orbit. In Figure 6, we show a calculation of the radiation damage to the solar cells on the COMETS mission. SAVANT uses the AP-8 and AE-8 models for particle flux, and the displacement damage dose method to calculate radiation damage.[11] We see good agreement between the calculation and data until about day 350, when other processes began to affect the solar arrays.

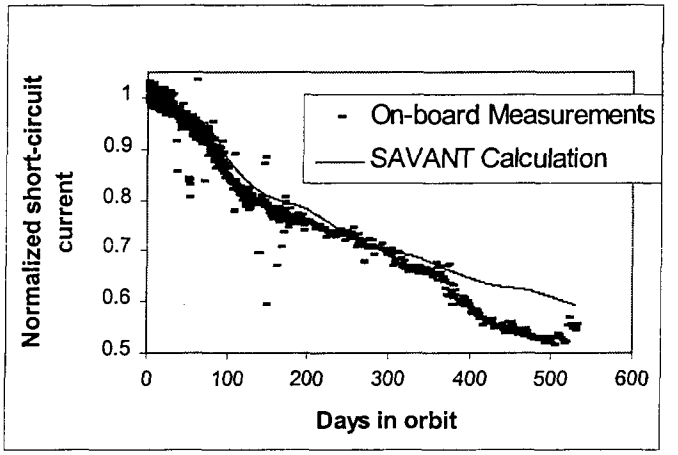

Figure 6 - C radiation damage, compared to SAVANT calculation

3. Comparison to other space flights

However, there are a number of problems with AP-8 and AE-8. Fundamentally, they do not show any dynamic phenomena, and are based on an ordinary solar cycle. In addition, they use a fixed magnetic field of 1964 or 1970, which does not reflect the movement of the magnetic field (and therefore the radiation belts). Several missions have flown in the last 20 years which have measured the radiation flux, and they show significant deviations from the model predictions. We will show some results from the Combined Release and Radiation Effects Satellite (CRRES) and the APEX missions.

A more complete discussion of the CRRES mission can be found in Johnson and Kieren.[12] The results of the radiation measurements can be found in Gussenhoven, et. al.[13] The CRRES mission was launched on July 25, 1990. Its orbit of 350 x 35,000 km, 18.1 degree inclination carried it through the heart of the radiation belts. It was equipped with over 40 instruments to measure the radiation environment, and its effects on electronics.

The CRRES data were separated into different L and B/B_0 bins, which allowed a direct comparison to AE-8 and AP-8. The CRRES data were further separated into categories of high and low magnetic activity. As seen in Figure 7, the AE-8 models overestimates the electron density for altitudes less than about 6000 km. Above that, the high magnetic activity data agree with AE-8, but both are higher than the low magnetic activity data, until about 20,000 km, when AE-8 overestimates both. The AE-8

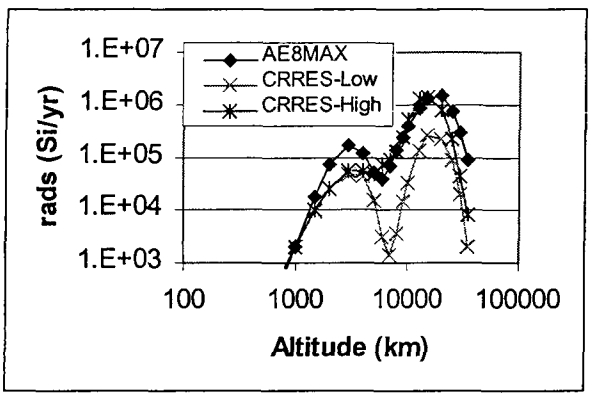

Figure 7 - Comparison of AE-8 to CRRES measurements.

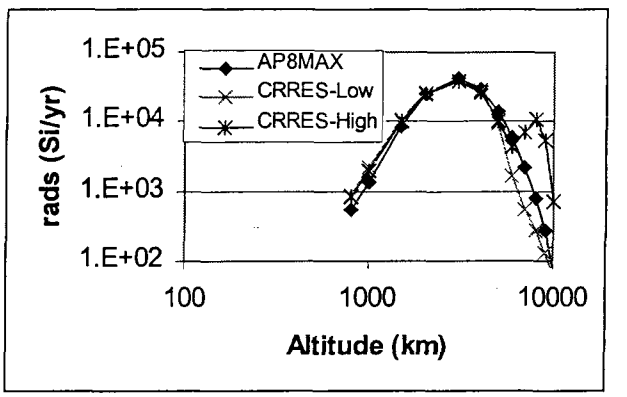

Figure 8 - Comparison of AP-8 to CRRES measurements.

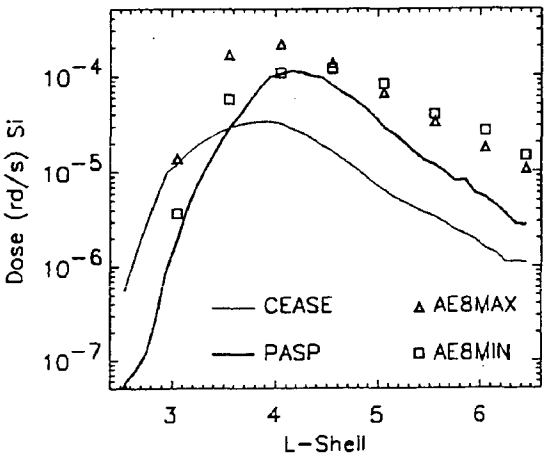

Figure 9 - Comparing two flight experiments to AE-8.

measurements include a nuclear explosion (Starfish) in 1964, which generated excess electrons in the environment, and those excess electrons were measured as late as eight years later.

In contrast, the proton environment shows little difference between high and low magnetic activity up to about 6000 km. Both data sets confirm the AP-8 predictions to that altitude. Above that, the AP-8 falls between the two datasets. Given the new radiation belt seen (discovered?) by CRRES, this is not a large surprise.

Brautigam, et. al,[14] have discussed the variation of the electron radiation belts with solar cycle. They compare the electrons detected by two experiments. The PASP experiment on the APEX spacecraft, operated from 1994 until 1996, a solar minimum cycle. The CEASE experiment, on the TriService Experiment 5 (TSX5), was launched on June 7, 2001, a solar maximum time. As with the CRRES data, the electron measurements were sorted by L and B/B0 bins, to compare with AE-8, as well as the CRRES-ELE models.

We see their results in Figure 9. The PASP measurements from solar minimum are as much as an order of magnitude lower than the AE-8MIN predictions for L larger than 4. However, the CEASE measurements are substantially different from the AE-8MAX predictions.

It is important to remember we haved compared dynamic data to the static NASA models. As a final comparison, we turn to Daly, et. al.[15] They discuss results from proton and electron detectors on STRV-1, which flew in a geosynchronous transfer orbit for almost four years. We look at three years of their data for electron detectors, and two years of their proton detector data in Figure 10.

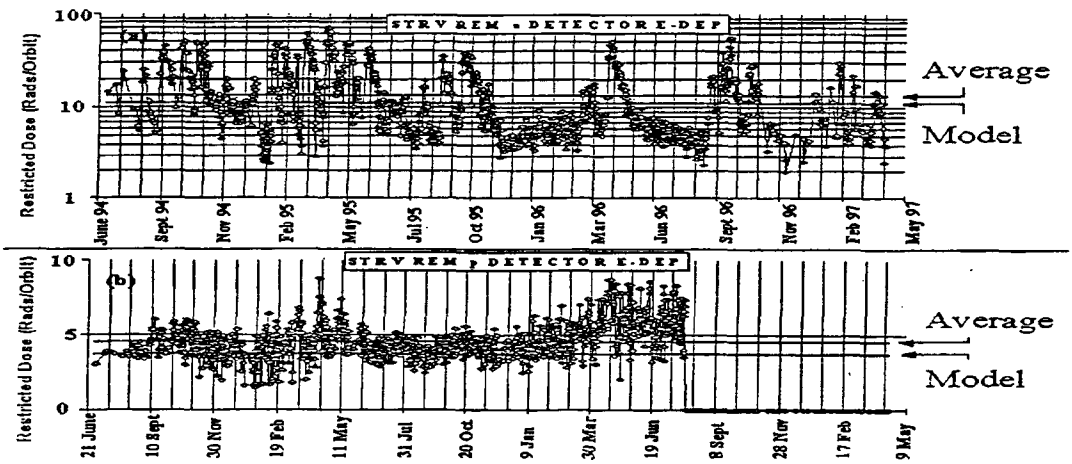

Figure 10 - Data from STRV electron and proton detectors, compared to AP-8 + AE-8 model predictions.

We see that both channels show a large dynamic range (note that the top scale is logarithmic), but that the average detector reading exceeds the AP-8 + AE-8 prediction by only about 20%. They need to use a sum of the two models, because both detectors see both types of particles, but predominantly see electrons or protons.

4. Conclusions

Clearly, there is a need for improved models of the trapped radiation belts. Within the last ten years, the US Air Force has been developing a model based on the CRRES data. However, this is limited to a smaller range of L and B/B_0 numbers than the AP-8 and AE-8 models. It is also restricted to solar maximum conditions, as it is based solely on the CRRES data-set. CRRES was operational for only 14 months.

NASA is supporting an effort to improve the AP-8 and AE-8 models, but progress has been slow. Whereas 45 satellites were flown with particle detectors in the early space-age, only a few have had particle detectors in the last ten years. This has restricted the coverage of those satellites, which had hindered the development of the models.

There are two low-altitude proton models in progress. Daniel Heynderickx of ESA has developed a model based on the Proton/Electron Telescope on the SAMPEX spacecraft.[16] It is available for use at the SPENVIS web-site.[17] Stu Huston of Boeing is working on a different model, based on data from almost 20 years of data from the TIROS/NOAA satellites.[18] However, this model is not generally available yet, and models protons in only a limited energy range.

Thus, the AP-8 and AE-8 models, which have been available for 30 years, remain the default radiation environments, only because they provide the largest coverage, and are available to the international public. Even so, there is useful information in the AP-8 and AE-8 models, and they continue to provide a point of comparison for radiation measurements on spacecraft. Hopefully, in the coming years, we will see improved models of the radiation environment.

5. Acknowledgements

This work was sponsored by NASA Glenn Cooperative Agreement NCC3-801. The author would also like to express his thanks to Sumio Matsuda and Mitsuru Imaizumi for their gracious invitation to attend this conference.

[1] J. Barth,, 1997 Nuclear and Space Radiation Effects Conference (NSREC) Short Course.
[2] J. Mazur, 2002 NSREC Short Course.
[3] C. McIlwain, Journal of Geophysical Research, Vol. 66, p. 3681, 1961.
[4] See http://nssdc.gsvc.nasa.gov/space/model/.
[5] D.M. Sawyer and J.I. Vette, "AP-8 Trapped Proton Environment for Solar Maximum and Solar Minimum", NSSDC/WDC-A-R&S, 76-06, NASA/Goddard Space Flight Center, Greenbelt, MD, December, 1976.
[6] J.I. Vette, "AE-8 Trapped Electron Model Environment", NSSDC/WDC-A-R&S, 91-24, NASA/Goddard Space Flight Center, Greenbelt, MD, November, 1991.
[7] N. Peddie, Journal of Geomagnetism an Geoelectricity, Vol. 34, p. 309, 1982.
[8] See http://nssdc.gsfc.nasa.gov/space/model/magnetos/igrf.html.
[9] From http://science.msfc.nasa.gov/ssl/pad/solar/images.
[10] O. Anzawa, K. Aoyama, T. Aburaya, K. Shinozaki, S. Matsuda, T. Ohshima, I. Nashiyama, H. Ito, S. Okada, T. Nakao, and Y. Matsumoto, "Flight Data of GaAs Solar Cells on the COMETS", Proc. Space Photovoltaic Research and Technology XVI Conference, August, 1999.
[11] S. R. Messenger, R. J. Walters, G. P. Summers, T. L. Morton, G. La Roche, C. Signorini, O. Anzawa and S. Matsuda, "A Displacement Damage Dose Analysis of the COMETS and Equator-S Space Solar Cell Flight Experiments", Proc. 16th European Photovoltaic Solar Energy Conference. May 3, 2000.

[12] M. H. Johnson and J. Kierein, J. Spacecraft and Rockets, V. 29, p 556, 1992.
[13] M. S. Gussenhoven, E. G. Mullen, and D. H Brautigam, IEEE Trans. Nuc. Sci. Vol. 43, p. 353, 1996.
[14] D. H. Brautigam, D. K. Dichter, K. P. Ray, W. R. Turnbull, D. Madden, A. Ling, E. Holeman, R. H. Redus, and S. Woolf, IEEE Trans Nuc. Sci., Vol. 48, p. 2010, 2001.
[15] E. J. Daly, P. Buhler, and M. Kruglanski, IEEE Trans. Nuc. Sci. Vol. 46, p. 1469, 1999.

[16] D. Heynderickx, M. Kruglanski, V. Pierrard, J. Lemaire, M.D. Looper, and J. B. Blake, IEEE Trans Nuc. Sci., Vol. 46, p. 475, 999.
[17] See http://www.spenvis.oma.be/spenvis/.
[18] S. L. Huston and K.A Pitzer, IEEE Trans. Nuc. Sci. Vol. 45, p. 2972, 1998.